Human mitochondrial RNA decay mediated by PNPase–hSuv3 complex takes place in distinct foci

Lukasz S. Borowski[1], Andrzej Dziembowski[1,2], Monika S. Hejnowicz[2], Piotr P. Stepien[1,2] and Roman J. Szczesny[1,2,*]

[1]Institute of Genetics and Biotechnology, Faculty of Biology, University of Warsaw and [2]Institute of Biochemistry and Biophysics, Polish Academy of Sciences, Pawinskiego 5a, 02-106 Warsaw, Poland

ABSTRACT

RNA decay is usually mediated by protein complexes and can occur in specific foci such as P-bodies in the cytoplasm of eukaryotes. In human mitochondria nothing is known about the spatial organization of the RNA decay machinery, and the ribonuclease responsible for RNA degradation has not been identified. We demonstrate that silencing of human polynucleotide phosphorylase (PNPase) causes accumulation of RNA decay intermediates and increases the half-life of mitochondrial transcripts. A combination of fluorescence lifetime imaging microscopy with Förster resonance energy transfer and bimolecular fluorescence complementation (BiFC) experiments prove that PNPase and hSuv3 helicase (Suv3, hSuv3p and SUPV3L1) form the RNA-degrading complex *in vivo* in human mitochondria. This complex, referred to as the degradosome, is formed only in specific foci (named D-foci), which co-localize with mitochondrial RNA and nucleoids. Notably, interaction between PNPase and hSuv3 is essential for efficient mitochondrial RNA degradation. This provides indirect evidence that degradosome-dependent mitochondrial RNA decay takes place in foci.

INTRODUCTION

RNA turnover plays a fundamental role in the regulation of gene expression, and it is mediated by protein complexes, such as the bacterial degradosome, the yeast mitochondrial degradosome or the eukaryotic nuclear or cytosolic exosomes (1–4). Moreover, RNA degradation is often spatially organized. For example, in the cytoplasm of eukaryotic cells, distinct foci called P-bodies are involved in RNA turnover (5). In human mitochondria, the enzyme responsible for RNA degradation has not been identified so far, and nothing is known about spatial organization of the RNA decay machinery.

Human mitochondrial DNA (mtDNA) is a circular double-stranded DNA molecule, which is organized into mitochondrial nucleoids containing mtDNA together with proteins involved in its metabolism (6,7). The genome contains 37 genes coding for 13 proteins, two ribosomal RNAs (rRNAs) and a set of 22 transfer RNAs (tRNAs), which generally flank other genes. During expression of mitochondrial genetic information, both strands of mtDNA (H-heavy and L-light) are transcribed into long polycistronic transcripts, which are processed by endoribonucleases acting at tRNA sequences (8–11). Such processing results in the formation of mature messenger RNAs (mRNAs), rRNAs, tRNAs and large amounts of non-coding RNA complementary to mRNAs and rRNAs, which are immediately removed (12). Thus, RNA decay is not only involved in the regulation of gene expression by regulating the levels of functional RNAs but also, in addition, is necessary for degradation of RNA-processing by-products and removal of potentially toxic malformed RNA molecules. Therefore, the identification of the enzyme responsible for mitochondrial RNA (mtRNA) decay is essential for understanding the aforementioned processes in human mitochondria.

In *Saccharomyces cerevisiae*, mtRNA decay is performed by a two-subunit complex called the mitochondrial degradosome, which consists of RNA helicase Suv3 and hydrolytic exoribonuclease Dss1 (13–16).

In contrast to yeast, plant mtRNA is degraded by polynucleotide phosphorylase (PNPase) (17). PNPase catalyzes processive 3′ to 5′ phosphorolysis of RNA and the reverse reaction, in which nucleoside diphosphates serve as substrates for elongation of the 3′ end of RNA (18). Plant mitochondrial PNPase takes part in degradation of rRNA and tRNA-processing intermediates,

*To whom correspondence should be addressed. Tel: +48 2 25 92 20 24; Fax: +48 2 26 58 41 76; Email: rszczesny@ibb.waw.pl

non-coding RNA transcribed from intergenic regions and antisense RNA (17).

Human *PNPase* was initially identified as a gene up-regulated in terminal cellular differentiation and senescence (19), and it was found to localize to mitochondria (20). In *Escherichia coli*, PNPase is a component of the degradosome, the complex responsible for degradation of polyadenylated RNAs, which consists of PNPase, ribonuclease (RNase) E, the RhlB helicase and the glycolytic enzyme enolase (21). Bacterial PNPase forms a homotrimeric complex with a ring-like structure surrounding the central channel through which single-stranded RNA is threaded (22,23). Similarly, human PNPase was found to exist as a homotrimer (24).

Mammalian mtRNA stability factors are largely undefined. The best known one is the LRPPRC–SLIRP complex (25–27). However, none of its components have enzymatic activity required for RNA degradation. So far, the human ortholog of yeast Suv3 helicase (hSuv3) is the only enzyme that has been shown to be directly involved in mtRNA decay. Silencing of *hSUV3* expression or induction of an exogenous hSuv3^{G207V} dominant-negative mutant in human cells results in increased stability of mature mRNAs and the accumulation of RNA species not observed under normal conditions because of their rapid removal or low abundance, i.e. mtRNA decay intermediates, aberrantly formed RNAs, processing by-products and vast amounts of non-coding antisense RNA (28).

In contrast to the well-documented involvement of hSuv3 helicase in mtRNA degradation, the identity of its ribonucleolytic partner is still unknown. As there is no human ortholog of the yeast Dss1 RNase, we considered PNPase as potential interactor of hSuv3. We have reported co-purification of both proteins from human mitochondria (28). On the other hand, PNPase was shown to be present in the mitochondrial inter-membrane space (IMS) (29), where it functions in RNA import into mitochondria (30). Moreover, silencing of *PNPase* led to conflicting results, not necessarily suggesting the involvement of this enzyme in mtRNA metabolism (29,31,32).

Here, we show that human mtRNA degradation is mediated by a PNPase–hSuv3 complex that occurs in distinct foci. We demonstrate that silencing of *PNPase* has a similar effect on accumulation of undegraded RNA decay intermediates as does dysfunction of hSuv3 (28). We present data that prove the *in vivo* interaction of PNPase and hSuv3. Notably, formation of the complex is necessary for mtRNA degradation. Our results indicate that the RNase PNPase and the helicase hSuv3 together form the human mitochondrial degradosome.

MATERIALS AND METHODS

Cell culture and siRNA transfection

HeLa, 143B or 293 T-Rex cells (Invitrogen) were grown as a monolayer at 37°C, under 5% CO_2 in DMEM medium (Gibco) supplemented with 10% FBS (Gibco) or TET System Approved FBS (Clontech) in case of stable inducible cell lines. Silencing of *PNPase* gene was performed using stealthRNA and Lipofectamine RNAiMAX according to the manufacturer's instructions (Invitrogen). The stealthRNA oligo ID HSS131758 (named si1), HSS131759 (si2) and negative control (Stealth^{TM} RNAi Negative Control Med GC) were used at a final concentration of 20 nM. Cells were plated 2 days after transfection and collected after 2 additional days of culturing. Expression of exogenous genes was induced by addition of tetracycline to the culture medium at a concentration of 25 ng/ml.

DNA cloning and establishment of stably transfected cell lines

DNA cloning was performed using standard procedures and described in Supplementary Data together with the establishment of stable cell lines. All constructs are listed in Supplementary Table S1.

Western blotting

Protein samples were prepared and processed as described previously (28). Used antibodies are listed in Supplementary Data.

Northern blot analysis

Total RNA was isolated by TRI Reagent (Sigma) using the manufacturer's protocol and analyzed essentially, as described previously (28). For details see Supplementary Data.

RNA half-life calculation

Newly transcribed RNA in cells treated with stealthRNA (specific for *PNPase* gene or negative control) was metabolically labeled by culturing cells for 1 h in the presence of 250 µM 4-thiouridine (4sU) (Sigma). Total RNA was isolated by TRI Reagent (Sigma); 100 µg of RNA was biotinylated in RNase free Biotinylation Buffer (10 mM Tris, pH 7.4) for 1.5 h with rotation; 2 µg of biotin (EZ-Link Biotin-HPDP, Catalog No. 21341) per 1 µg of RNA was used. RNA was extracted by chloroform/isoamyl alcohol (24:1) and precipitated with 0.5 M NaCl and isopropanol. After dissolving in water, the RNA was heated to 65°C for 10 min, then placed on ice for 5 min and incubated with streptavidin-coupled Dynabeads^{TM} (Invitrogen) for 15 min with rotation at room temperature, as described in Dolken *et al.* (33). Beads were separated from solution using a magnet stand; solution containing unbound RNA was stored at −80°C (un-labeled fraction—pre-existing RNA). Beads were washed three times with washing buffer (100 mM Tris, pH 7.5; 10 mM EDTA; 1 M NaCl and 0.1% Tween20) heated to 65°C and three times with the same buffer at room temperature. RNA bound to beads (labeled fraction—newly synthesized RNA) was eluted from beads with 100 mM dithiothreitol in RNase-free water and recovered with RNeasy mini columns (Qiagen) according to the manufacturer's instructions and stored in −80°C. A total of 1.5–2 µg of RNA was dissolved in denaturing solution and run on a 1% agarose gel, as described

previously (28). For quantification of pre-existing and total RNA amount, northern blot analysis was performed with riboprobes specific for transcripts: ND2, ND3, CytB, COX2, mirror-COX1 (labeled with [α-^{32}P] UTP on the template of a polymerase chain reaction [PCR] products listed in Supplementary Information). For standardization, filters were re-probed with a 7SL probe (28). Autoradiograms were collected, and signal intensity was counted by Multi Gauge V3.0 software (FujiFilm). RNA half-life calculations were based on the ratio of pre-existing RNA to total RNA, as described in (33). To obtain the final ratios, we applied in the equation the correction factor described by Dolken *et al.* (33).

Protein purification

Mitochondria were isolated as described previously (28). The following procedure was performed at 4°C. Just before lysis, mitochondria isolated from cells expressing PNPase-FLAG were mixed with mitochondria from cells expressing hSuv3-TAP in the ratio of 1:3. This ratio was chosen because of the higher expression of PNPase-FLAG in comparison with endogenous PNPase. Mitochondrial extracts were cleared by centrifugation, mixed with IgG Sepharose (GE Healthcare) and incubated for 1.5 h with rotation. If indicated, RNase A was added at this step to obtain a final concentration of 40 μg/ml. After incubation, resins were extensively washed with IPP 150 buffer and TEV cleavage buffer. Proteins were eluted by treatment with TEV protease for 2 h at 18°C. Collected eluates were analyzed by western blotting.

Fluorescence lifetime imaging microscopy-Förster resonance energy transfer (FLIM-FRET) and bimolecular fluorescence complementation (BiFC) analysis

HeLa cells analyzed by fluorescence lifetime imaging microscopy-Förster resonance energy transfer (FLIM-FRET) were grown on Lab-Tek^{TM} II Chamber Slides^{TM} (Nunc). Cells were transiently transfected using the TransIT® LT2020 reagent (Mirus) according to the manufacturer's instructions. A total of 50 ng of each DNA construct and 7000 cells were used per transfection. Following 24 h of incubation, cells were imaged with a FluoView1000 confocal microscope (Olympus) with a Compact Lifetime and FCS Upgrade Kit (PicoQuant) on an inverted IX81 microscope, using a PLANAPO 60.0 × 1.40 oil objective. PNPase-EGFP fusion protein was excited by a 483-nm pulsing laser. Image analysis was performed with the SymphoTime software (PicoQuant). For bimolecular fluorescence complementation (BiFC) analysis, HeLa cells were plated in six-well plates to get a confluence of 40–50% at the time of transfection. Cells were transfected with 500 ng of each DNA construct (pRS407/pRS412, pRS408/pRS412, pRS409/pRS411 and pRS410/pRS411) with usage of TransIT® LT2020 reagent (Mirus). Twenty-four hours later, cells were passaged to Lab-Tek^{TM} II Chamber Slides^{TM} (Nunc) and analyzed for the following additional 24 h. Before imaging cells, mitochondria were labeled with MitoTracker Orange CMTM-Ros (0.1 μM) (Molecular Probes) and analyzed

using a FluoView1000 confocal microscope (Olympus) with a PLANAPO 60.0 × 1.40 oil objective. The 3D reconstructions were done using Imaris 7.2.3 software (Bitplane).

Immunofluorescence

HeLa or 143B cells were plated on glass cover slips for 24 h, then transfected with BiFC DNA constructs using the TransIT® LT2020 reagent (Mirus). After 1 day of culturing, cells were fixed with 4% formaldehyde and subjected to the immunostaining procedure described previously (28). If needed, RNA was labeled by the addition of bromouridine (BrU) (2.5 mM) (Sigma) to the culture medium 20 min before fixation. Mitochondria were stained by addition of MitoTracker DeepRed (0.25 μM) (Molecular Probes) to the culture medium 20 min before fixation. PNPase-C-Venus was detected with goat polyclonal anti-GFP antibodies (I-16, sc-5385, Santa Cruz); RNA was detected with rat monoclonal anti-BrdU antibodies (ab6326, Abcam) and DNA was stained with anti-DNA mouse monoclonal IgM antibodies (ProGen). Suitable secondary antibodies conjugated with Alexa488, Alexa555 and Alexa635 (Molecular Probes) were used to exclude cross-hybridization and fluorescence cross-talk when used in combination. Cells were imaged as described earlier. The 3D reconstructions and spots measurements were carried out using Imaris 7.2.3 software. Spots, whose centers were distant from 0 up to 0.25 μm (optical resolution of the microscopic system was estimated at 0.215 μm while images were collected), were deemed to be co-localized. Focal adjustment of the confocal microscope was tested using FocalCheck^{TM} fluorescence microscope test slide #1 (F36909, Molecular Probes). These tests clearly showed proper adjustment of the microscopy system (Supplementary Figure S1).

Quantification of adenosine triphosphate (ATP) in mitochondria

Mitochondria from cells with silenced PNPase or cells expressing hSuv3 were isolated, as described previously (28). Adenosine triphosphate (ATP) levels in mitochondria were analyzed using Luminescent ATP Detection Assay Kit (ab113849, Abcam) according to the manufacturer's instructions.

ATP depletion and quantification

To decrease cellular ATP levels, 293 T-Rex cells were treated with a mixture of 2-deoxy-D-glucose (10 mM, D6134, Sigma) and 50 μM carboxyatractyloside potassium salt (C4992, Sigma) or sodium azide (3.5 or 5 mM, Sigma). Cells were collected after 2, 6, 12 and 24 h of treatment. Cellular ATP levels were quantified using Luminescent ATP Detection Assay Kit (ab113849, Abcam) according to the manufacturer's instructions.

RESULTS

PNPase depletion stabilizes mitochondrial transcripts

Careful inspection of the human nuclear genome did not suggest many proteins with an exoribonuclease fold and with a putative mitochondrial targeting signal other than PNPase. This prompted us to analyze whether PNPase could be involved in human mtRNA decay. We checked the effect of *PNPase* gene silencing on mtRNAs stability. Four mRNAs (ND2, ND3, CytB and COX2) and one non-coding RNA were analyzed. The mRNAs represent transcripts that encode subunits of different complexes of the electron transport chain and are encoded by genes localized in different parts of the mitochondrial genome.

We constructed a stable 293 T-Rex cell line (293^{PNP_si1Res}) carrying the *PNPase* gene with silent mutations in the sequence complementary to an siRNA that targets the native PNPase mRNA for destruction. In this way, the exogenous gene expression induced by tetracycline was resistant to siRNA silencing, while the native *PNPase* gene expression could be silenced by the same siRNA. Cells were transfected with control siRNA or siRNA against PNPase. Four days post-transfection, newly synthesized RNA was metabolically labeled by 4sU incorporation. Subsequently, RNA was isolated from the cells, biotinylated and separated on streptavidin beads to separate total RNA into newly synthesized and pre-existing fractions (Figure 1A). The ratio of the amount of pre-existing RNA to total RNA allows the calculation of the RNA half-life (33).

Our results indicate that in cells transfected with siRNA against PNPase and not expressing the exogenous *PNPase*^{si1Res} gene, the half-lives of all analyzed RNAs increased, although to different extents, compared with cells treated with control siRNA (Figure 1B). On induction of an exogenous *PNPase* mutant gene resistant to siRNA, the half-lives levels of transcripts were brought back to the control levels (Figure 1B). As the experimental procedure does not allow the determination of the efficiency of silencing at the protein level, we checked this in parallel experiments (see later).

Stabilization of tested mtRNAs on *PNPase* silencing, as well as the fact that we reproducibly observed a pool of PNPase resistant to proteinase K treatment in digitonin-prepared human mitoplasts (Supplementary Figure S2), which indicates its matrix localization, suggested that the protein may be involved in mtRNA degradation. This prompted us to perform further studies.

Silencing of PNPase leads to accumulation of RNA degradation intermediates transcribed from H- and L-strands

Previously, we showed that disruption of hSuv3 function results in accumulation of RNA degradation intermediates (28). We expected that if PNPase is participating in mtRNA decay, a similar phenotype should be observed. To check this, two stable human 293 cell lines (293^{PNP_si1Res} and 293^{PNP_si2Res}) containing inducible re-coded *PNPase* genes resistant to siRNA silencing were transfected with two different siRNAs against PNPase (si1 and si2). The efficiency of endogenous native PNPase silencing was checked by western blotting. Transfection of cells with both si1 and si2 led to a strong depletion of PNPase (Figure 2A). In contrast, the level of PNPase variants resistant to silencing was not changed (Figure 2A). To examine whether the
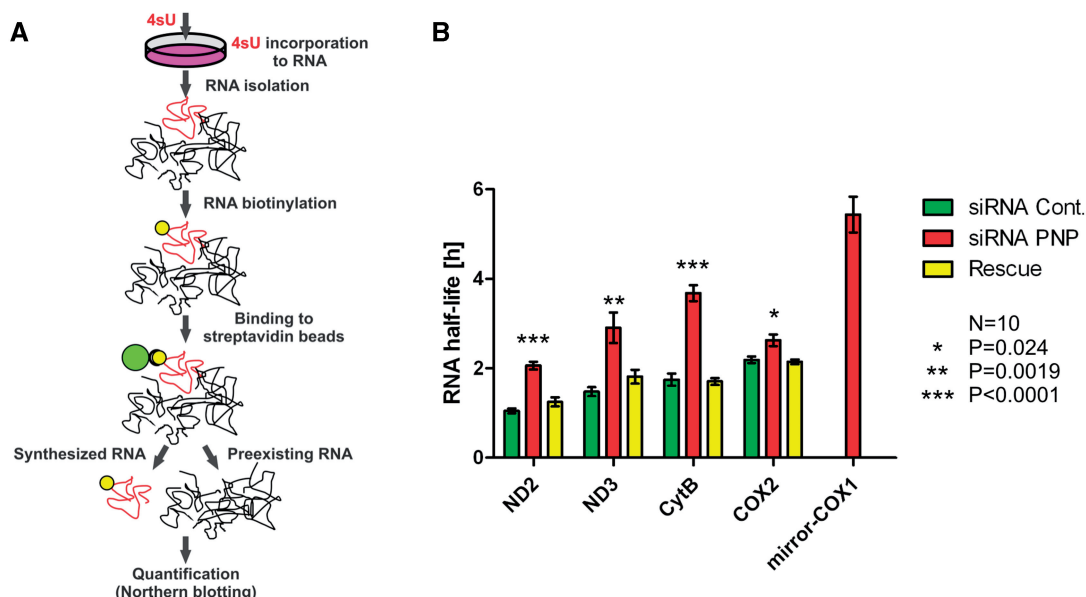

Figure 1. PNPase depletion stabilizes mitochondrial transcripts. (**A**) Schematic representation of the RNA half-life measurement, details in the text. (**B**) Graph representing quantified RNA half-lives of the mitochondrial transcripts. The mean values obtained in 10 independent experiments are presented. Error bars represent standard deviation. The *P*-values were obtained in an ANOVA test. Quantification of the half-life of mirror COX1 in cells transfected with control siRNA or rescued by expression of exogenous PNPase was impossible because of its low abundance.
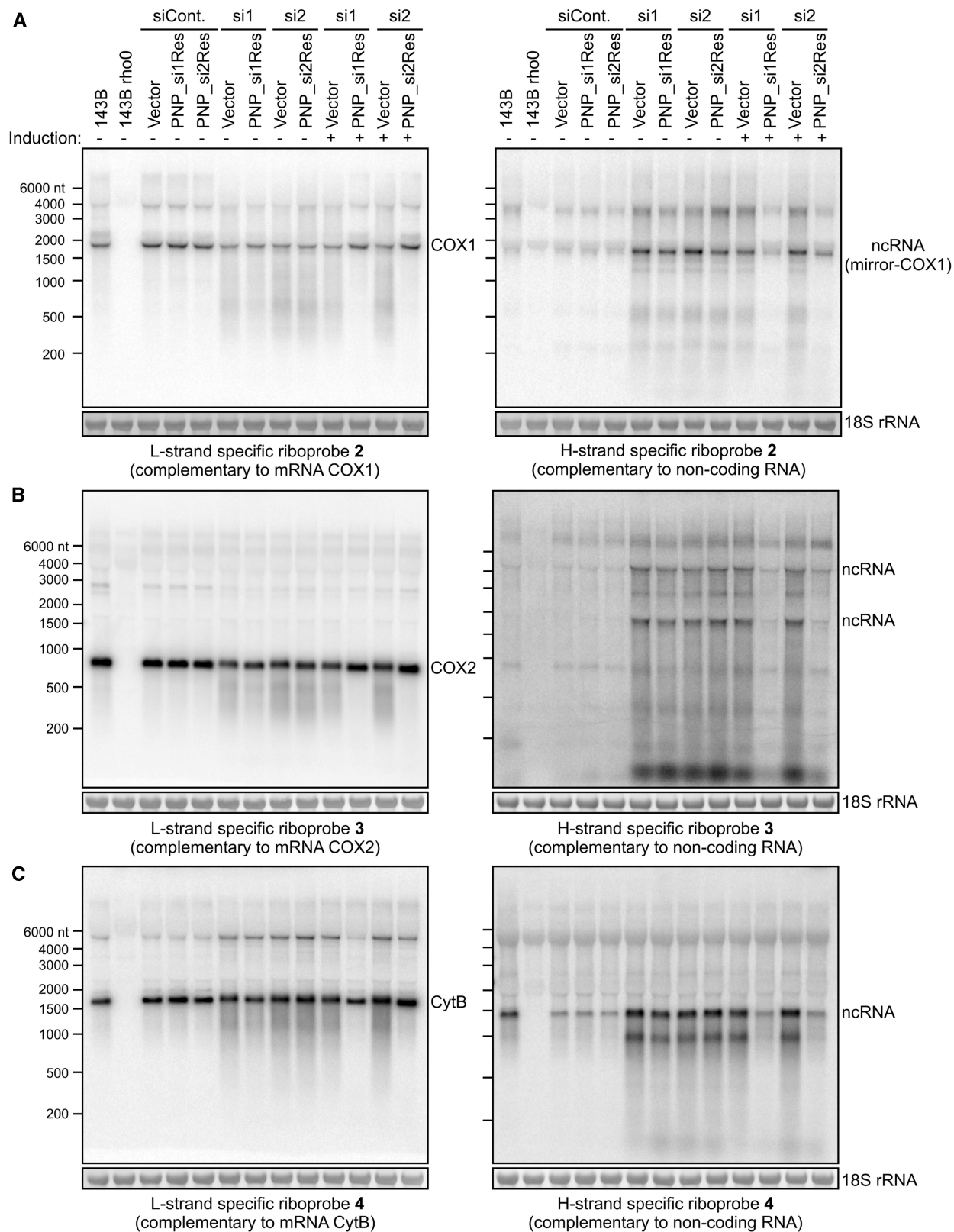
Figure 2. Silencing of PNPase leads to accumulation of mtRNA degradation intermediates. Stable cell lines (PNP_si1Res, PNP_si2Res) that express inducible PNPase resistant to siRNA anti-PNPase or control cell line having integrated empty vector was transfected with two different siRNAs specific for PNPase (si1 and si2) or control siRNA. Expression of exogenous PNPase was induced by tetracycline at the transfection point. Cells were collected 4 days post-transfection and analyzed by western and northern techniques. (**A**) Western blot analysis of the PNPase and hSuv3 levels, as standardization actin staining was performed. (**B**) Schematic representation of the polycistronic RNA resulting from H- or L-strand transcription and localization of the used riboprobes. (**C**) Northern blot analysis using strand-specific riboprobes. Some hybridization signal was unspecific (especially from cytoplasmic rRNA). This was controlled using RNA isolated from 143B rho⁰ (devoid of mtDNA) and their parental 143B cells. Cytosolic 18S rRNA staining by methylene blue is shown as a loading control.
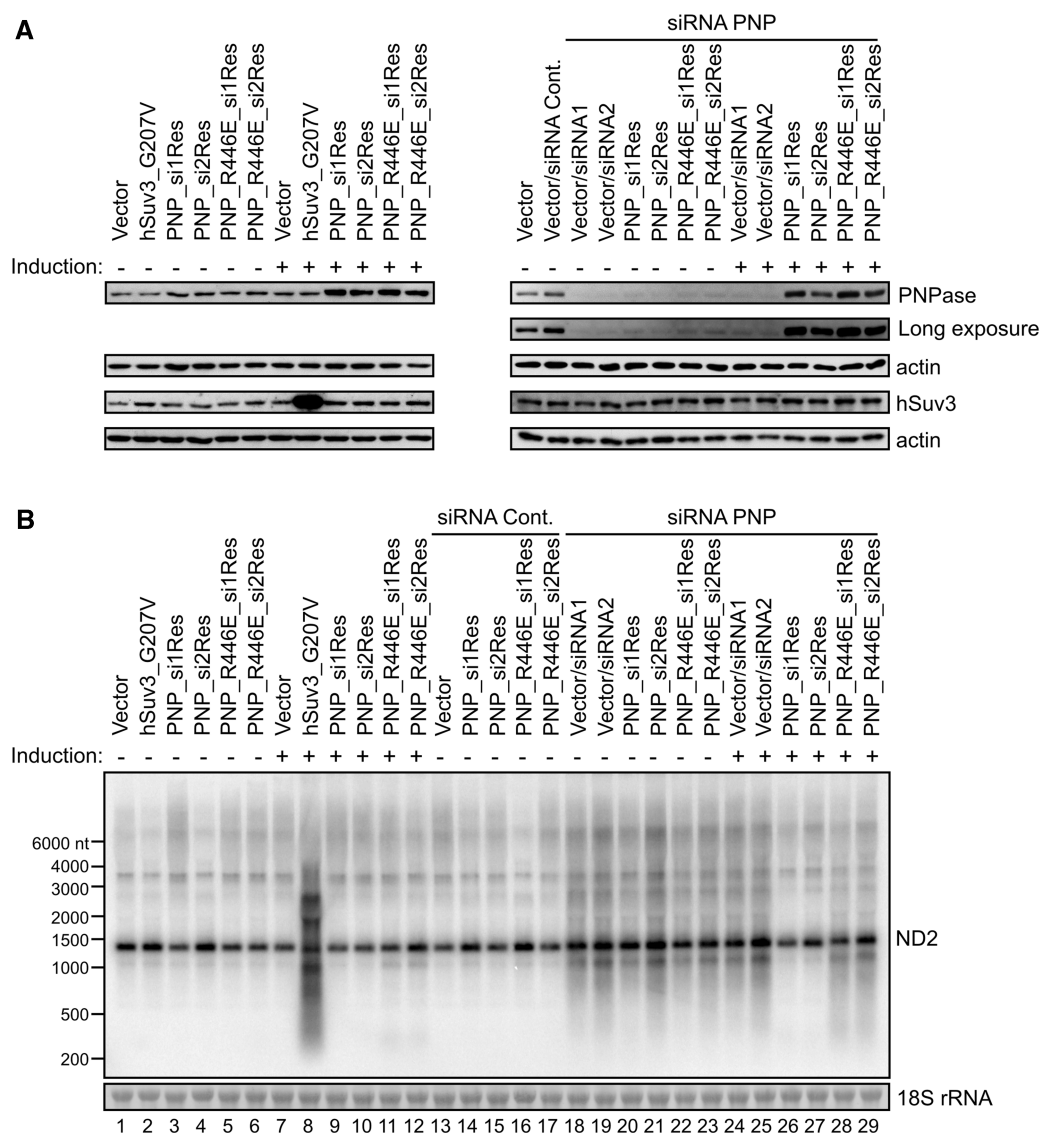
potential effects on mtRNA could be due to the changes in hSuv3 levels resulting from an off-target effect of PNPase silencing, we tested the level of hSuv3 in PNPase-depleted cells. Western blot analysis showed that the reduction of PNPase expression does not change the hSuv3 levels (Figure 2A).

Northern blot hybridization using riboprobes detecting ND2, COX1, COX2, CytB and ND3 mRNAs revealed that silencing of PNPase led to significant accumulation of RNA smear, representing molecules shorter than mature transcripts (Figures 2C and 3, Supplementary Figure S3, left panels). A similar but far less pronounced effect was observed in the case of a probe detecting 12S rRNA (Supplementary Figure S3B, left panel). In addition, inhibition of PNPase expression was found to affect the levels of mature RNAs; this effect, however, depends on the transcript. No substantial effect on the levels of mature ND2 was observed (Figure 2C, left

panel), whereas the levels of ND3 increased (Supplementary Figure S3). A reduction of the steady-state level was detected for COX1, COX2, CytB mRNAs, 12S rRNA and tRNAs (Figure 3, Supplementary Figure S3, left panels). Lowering of the steady-state levels of mtRNAs seems to be in disagreement with the measured stabilization of mt-mRNAs observed on PNPase silencing. Several possible reasons for this are described in the discussion. However, it is worth nothing that similar contradictory results were observed by others for nuclear and cytoplasmic transcripts when the RNA-degrading machinery was disrupted in those organelles (34–41).

Importantly, hybridization to probes detecting RNAs complementary to the investigated RNAs, i.e. non-coding RNAs transcribed from the opposite DNA strand, revealed a strong accumulation of these RNA species (Figures 2 and 3, Supplementary Figure S3, right panels). All of these effects were abolished by

Figure 3. PNPase depletion affects mitochondrial mRNAs. Stable cell lines (PNP_si1Res, PNP_si2Res) that express inducible PNPase resistant to siRNA anti-PNPase or control cell line having integrated empty vector was transfected with two different siRNAs specific for PNPase (si1 and si2) or control siRNA. Expression of exogenous PNPase was induced by tetracycline at the transfection point. Cells were collected 4 days post-transfection and subjected to RNA isolation and northern blot analysis. Strand-specific riboprobes were used to detect mRNAs for COX1, COX2 and CytB (A, B, and C respectively, left panels) or their antisense counterparts (A, B, and C, right panels). Some hybridization signal was unspecific (especially from cytoplasmic rRNA). This was controlled using RNA isolated from 143B rho^0 (devoid of mtDNA) and 143B cells (parent of 143B rho^0). Cytosolic 18S rRNA staining by methylene blue is shown as a loading control.

Figure 4. Active PNPase is necessary for mitochondrial RNA degradation. Using two different siRNAs (si1 and si2), endogenous PNPase was depleted in stable cell lines that express inducible catalytic active PNPase resistant to siRNA (PNP_si1Res and PNP_si2Res) or its inactive counterpart (PNP_R446E_si1Res and PNP_R446E_si2Res). As a control, a stable cell line with integrated empty vector was used, and also, transfection with control siRNA was performed. The 293 cell line expressing catalytically inactive hSuv3 (hSuv3_G207V) was used for a comparison with an effect of PNPase dysfunction. Expression of inactive PNPase leads to a weak dominant-negative effect. (**A**) Western blot analysis of the PNPase and hSuv3 levels. For standardization, actin staining was performed. (**B**) Northern blot analysis of ND2 transcript, probe detecting RNA transcribed from both H- and L-strand of mtDNA, was used. Cytosolic 18S rRNA staining by methylene blue is shown as a loading control.

expression of the exogenous *PNPase* gene resistant to siRNA silencing (Figures 2 and 3, Supplementary Figure S3). However, this was not the case when the catalytically inactive PNPase[R446E] (42) was expressed (Figure 4B, lanes 28 and 29 versus lanes 26 and 27). This shows that the observed perturbations in mtRNA metabolism are because of the lack of RNA-degrading activity of PNPase.

Noticeably, the effects of PNPase silencing on mtRNA decay are similar to the effects of *hSUV3* silencing (28). Also, expression of the enzymatically inactive form of PNPase leads to a dominant-negative phenotype similar to that caused by expression of the mutated hSuv3[G207V] protein (28), although the accumulation of partially degraded RNA is not as strong (Figure 4B, lanes 11 and 12 versus lane 8).

Accumulation of transcripts on PNPase silencing, which most likely constitute degradation intermediates and can be removed only by active PNPase, led us to the conclusion that the function performed by PNPase is required for proper RNA decay in human mitochondria.

Interaction of PNPase with hSuv3 helicase is necessary for mtRNA degradation

Our previous studies revealed that PNPase co-purifies with hSuv3 and *vice versa* (28). In addition, *in vitro* binding of both proteins was reported, and it was shown that the deletion of five amino acids of hSuv3 (amino acids 510–514) inhibits interaction with PNPase *in vitro*, but it does not affect helicase activity of hSuv3 (43).

Exogenous overexpression of the catalytically inactive form of hSuv3 (hSuv3^{G207V}) has a dominant-negative effect (28), as it probably outcompetes the endogenous wild-type hSuv3 from its interactions with the putative ribonucleolytic partner(s). We assumed that if PNPase interacts with hSuv3 *in vivo*, the expression of inactive hSuv3, which is in addition incapable of interacting with PNPase, should abolish the dominant-negative phenotype. To verify this, we established two stable cell lines with inducible expression of active or inactive hSuv3, both of which lack residues 510→514 (WT/Δ510-514 and G207V/Δ510-514, respectively) responsible for *in vitro* hSuv3–PNPase interaction. In agreement with the data of Wang *et al.* (43), we found that PNPase indeed does not co-purify with our constructed hSuv3$^{Δ510−514}$-TAP during affinity purification (see later).

RNA isolated 3 days after induction of exogenous genes was analyzed on northern blots with probes for ND2 and COX2. In agreement with previous results, expression of full-length but enzymatically inert hSuv3 led to accumulation of heterogeneous transcripts, whereas overexpression of the wild-type *hSUV3* gene had no effect (Figure 5A). In contrast, expression of active or inactive variants of hSuv3, both bearing the deletion abolishing their interaction with PNPase, did not affect the levels of ND2 or COX2 mRNAs nor induced the accumulation of heterologous RNA (Figure 5A), although proteins with the deletion were overexpressed to the same extent as the full-length ones (Figure 5B). Thus, our data suggest that *in vivo* interaction of PNPase with hSuv3 is required for RNA degradation in human mitochondria.

PNPase and hSuv3 helicase form a stable complex *in vivo*

Although in many cases, pull-down experiments allow the demonstration of true interactions, this method is not devoid of false positive results (44). Therefore, we tested whether the interaction between PNPase and hSuv3 arises during the purification procedure.

To do so, we mixed mitochondria isolated from cells overexpressing hSuv3-TAP with mitochondria isolated from cells overexpressing PNPase-FLAG. After lysis of mitochondria, we performed affinity purification of hSuv3-TAP and then analyzed the extracts and elutions by western blotting with antibodies against PNPase or FLAG tag (Figure 6A). Comparison of the amount of detected proteins in mitochondrial lysates and purified fractions indicated that much less FLAG-tagged PNPase than endogenous PNPase co-purifies with hSuv3-TAP (Figure 6B, compare lane 2 with 5 and lane 8 with 11). This indicates that the complex of PNPase with hSuv3-TAP had existed before mitochondria were lysed; hence, it means that co-purification of these proteins is not an artifact of the method.

Also, by performing parallel purification of hSuv3$^{Δ510−514}$-TAP, we show that the deletion of residues 510–514 in hSuv3 indeed strongly inhibits interaction with PNPase (Figure 6B, compare lane 4 and 6). The interaction between hSuv3 and PNPase is not mediated by RNA because the same amount of PNPase
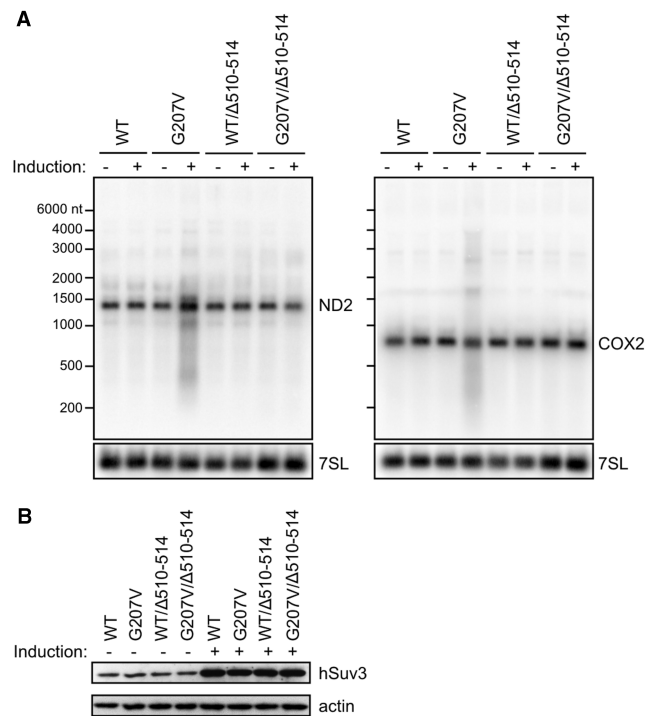

Figure 5. Deletion of residue 510–514 of hSuv3 disables PNPase–hSuv3 complex formation. Analysis of RNA isolated from stable 293 cell lines expressing, in an inducible manner, different forms of hSuv3 (WT: wild type, G207V: catalytically inactive, WT/Δ510-514: wild type with deletion of 510–514 residues and G207V/Δ510-514: catalytically inactive with deletion of 510-514 residues). Expression of exogenous hSuv3 by tetracycline is indicated. Cells were collected 3 days after induction and analyzed by northern and western blotting. (**A**) Northern blot analysis of ND2 and COX2 transcripts, probes detecting RNA transcribed from both H- and L-strand of mtDNA, were used. The level of 7SL is shown as a loading control. (**B**) Western blot analysis of the hSuv3 level. Actin staining was performed for standardization.

was purified with hSuv3-TAP regardless of the presence of RNase A (Figure 6C). This supports interaction between hSuv3 and PNPase *in vivo*.

To prove the formation of PNPase–hSuv3 complex *in vivo*, we used the FLIM-FRET technique. This method is based on a measurement of fluorescence lifetime of FRET donor protein (in this case fusion of PNPase with EGFP). An appearance of the energy transfer caused by protein–protein interactions shortens the fluorescence lifetime (45,46).

HeLa cells were transiently transfected with a plasmid encoding PNPase-EGFP fusion protein (FRET donor) or with a mixture of plasmids coding for PNPase-EGFP and hSuv3-mCherry (FRET acceptor). FLIM measurements were performed on living cells. Data analysis was corrected for the instrument response function and augmented by the maximum likelihood estimation algorithm. Acquired signals were color coded according to calculated average fluorescent lifetimes (Figure 7A). When PNPase-EGFP fusion was expressed alone, two fluorescent lifetimes of EGFP were calculated—1.1 and 2.7 ns (Figure 7A, left picture). Co-expression of both proteins, PNPase-EGFP and hSuv3-mCherry, resulted in
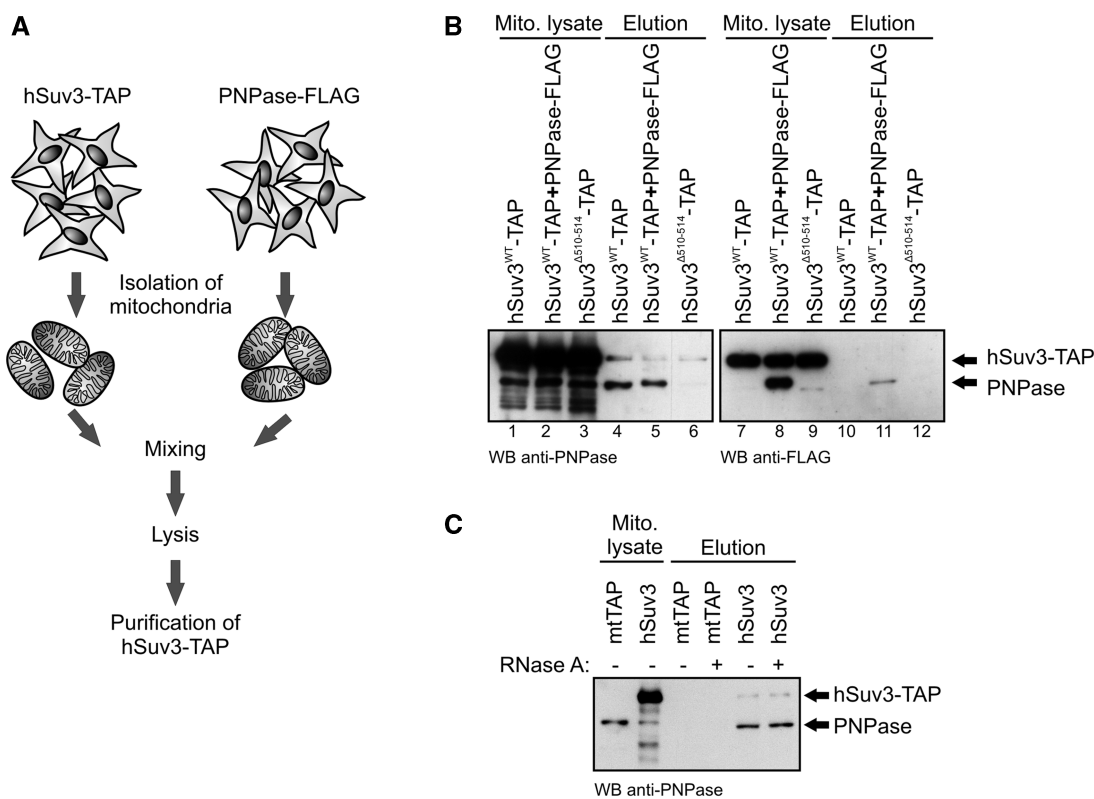
Figure 6. Co-purification of PNPase and hSuv3 helicase is not an artifact. (**A**) Schematic representation of the experiment. Mitochondria from 293 cells expressing hSuv3 or PNPase in fusion with the TAP or FLAG tag, respectively, were isolated, mixed together, lysed and chromatographic purification of hSuv3-TAP was performed. (**B**, **C**) Western blot analysis of the endogenous and exogenous PNPase levels in mitochondrial extracts and purified fractions obtained during hSuv3-TAP purification. Specific anti-PNPase or anti-FLAG tag antibodies were used. (C) The presence of RNase A during purification is indicated. The TAP-tagged hSuv3 protein is also detected because applied secondary antibodies produced in rabbit (B, left panel and C) or primary antibodies produced in mouse (B, right panel) bind directly to the protein A, which is a component of TAP tag.

appearance of regions with significantly shorter average fluorescent lifetime (Figure 7A, right picture, red spots), which indicates interaction of hSuv3 and PNPase *in vivo*. In most parts of the cell expressing FRET donor and FRET acceptor, we could calculate two fluorescent lifetimes (1.2 and 2.7 ns; Figure 7A, right picture, green area), which are similar to these calculated for donor-only sample (Figure 7A, left picture; see table for the results of calculations). In the regions with shortened average fluorescent lifetimes, we calculated two lifetimes—2.7 and a much shorter 0.4 ns (Figure 7A, right picture, red area). The longer one originates from the PNPase-EGFP donor molecules, which did not find a FRET acceptor partner. The 0.4-ns fluorescence lifetime consists of the quenched down long (2.7 ns) and short (1.2 ns) fluorescence lifetimes of the complete FRET molecules. Altogether these results indicate that in some regions of cells co-expressing PNPase-EGFP and hSuv3-mCherry, the lifetime of EGFP is much decreased, which is evidence of *in vivo* interaction of both proteins in these areas. Importantly, we found that EGFP tagging does not affect PNPase function because the wild-type fusion protein is capable of rescuing the silencing of native *PNPase* gene, but its inactive counterpart is not (Supplementary Figure S4, Supplementary Movies S1 and S2).

Careful analysis of the FLIM results indicated that fluorescent PNPase-EGFP molecules with shortened fluorescence lifetime were not randomly distributed throughout the mitochondrial network but concentrated in distinct regions. To study this in detail, we applied the BiFC method, as it sometimes permits higher spatial resolution than FLIM-FRET. The BiFC technique enables the investigation of proteins interaction by expressing them in fusion with unfolded complementary fragments of a fluorescent reporter [in our case a variant of YFP called Venus (47)]. If the studied proteins interact, they bring fluorescent protein fragments within proximity, which triggers its reconstitution and leads to emission of a fluorescent signal (48).

In agreement with the FLIM-FRET data, co-expression of PNPase and hSuv3 in a fusion with the C- and N-terminal part of Venus protein, respectively, resulted in fluorescence complementation in mitochondria of HeLa cells (Figure 7B and Supplementary Movies S3, S4 and S5). As presumed, the signal appeared only in spots. Importantly, the signal emitted by the PNPase–hSuv3$^{\Delta 510-514}$ pair, acquired at the same excitation and detection settings as the full-length proteins, was hardly visible (Supplementary Figure S5A).

On the basis of the described results, we concluded that in human mitochondria, PNPase and hSuv3 helicase form
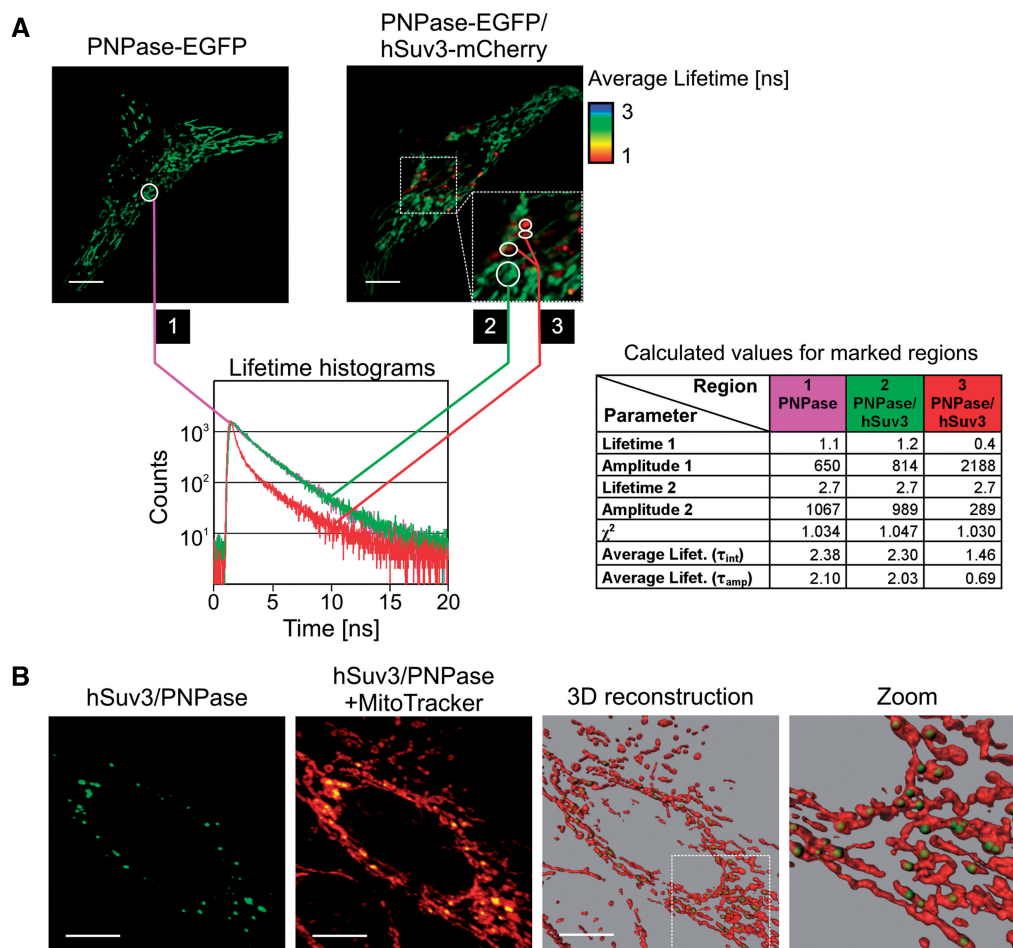
Figure 7. PNPase and hSuv3 helicase interact *in vivo*. (**A**) FLIM-FRET analysis of PNPase expressed in fusion with EGFP and hSuv3 expressed in fusion with mCherry. Images are color coded with respect to the average fluorescence lifetime of PNPase-EGFP. Fluorescence lifetime histograms obtained by time-correlated single photon counting generated for defined regions of the cells are presented. Calculated lifetimes and amplitudes are presented in the table. (**B**) BiFC analysis of hSuv3 and PNPase expressed in fusion with N- and C-terminal part of Venus, respectively. Mitochondria were visualized with MitoTracker Orange. The 3D reconstructions of fluorescence images are presented. The surface of mitochondria was made transparent to visualize PNPase–hSuv3 foci (A, B). Imaging of the living cells was performed. Bars represent 10 μm.

a stable mtRNA-degrading complex *in vivo*, which we shall call the mitochondrial degradosome.

The PNPase–hSuv3 complex is found in distinct foci and co-localizes with mtRNA and mtDNA

Previous and current experiments showed that both endogenous and exogenous expressed PNPase and hSuv3 are localized throughout the whole mitochondrial network (20,28,29,49,50). On the contrary, experiments using BiFC analysis clearly indicated fluorescence complementation only in well-defined distinct foci (Figure 7B).

To exclude the possibility that the observed foci are the result of unspecific behavior of the hSuv3 or PNPase in fusion with a part of Venus protein, we performed immunofluorescence analysis in HeLa cells, using anti-GFP antibodies specific to the C-terminal part of Venus protein. This revealed that even though PNPase-C-Venus fusion protein is present in whole mitochondria, the fluorescence complementation appears only in foci (Figure 8A). Expression of hSuv3-C-Venus and hSuv3$^{\Delta 510-514}$-C-Venus fusion proteins can also be

detected throughout mitochondria by immunofluorescence (Supplementary Figure S5B). However, the foci representing the interaction between PNPase-N-Venus and hSuv3-C-Venus are only detected when the wild-type variant of hSuv3 is used and not the deletion mutant incapable of interaction with PNPase (Supplementary Figure S5B).

These results indicate that only fractions of hSuv3 and PNPase pools interact, and that such interactions take place only in specific areas of mitochondria. Interestingly, it was shown that mtRNA also localizes in foci (51); however, their role has not been characterized yet. Therefore, we assumed that at least some of the mtRNA-containing foci may constitute mitochondrial degradation bodies. To study this issue, we examined whether the mitochondrial degradosome-containing foci co-localize with mtRNA.

The 143B osteosarcoma cells were transfected with plasmids enabling BiFC studies and cultured in the presence of BrU to label RNA, which can be subsequently detected using antibodies recognizing BrU. We also
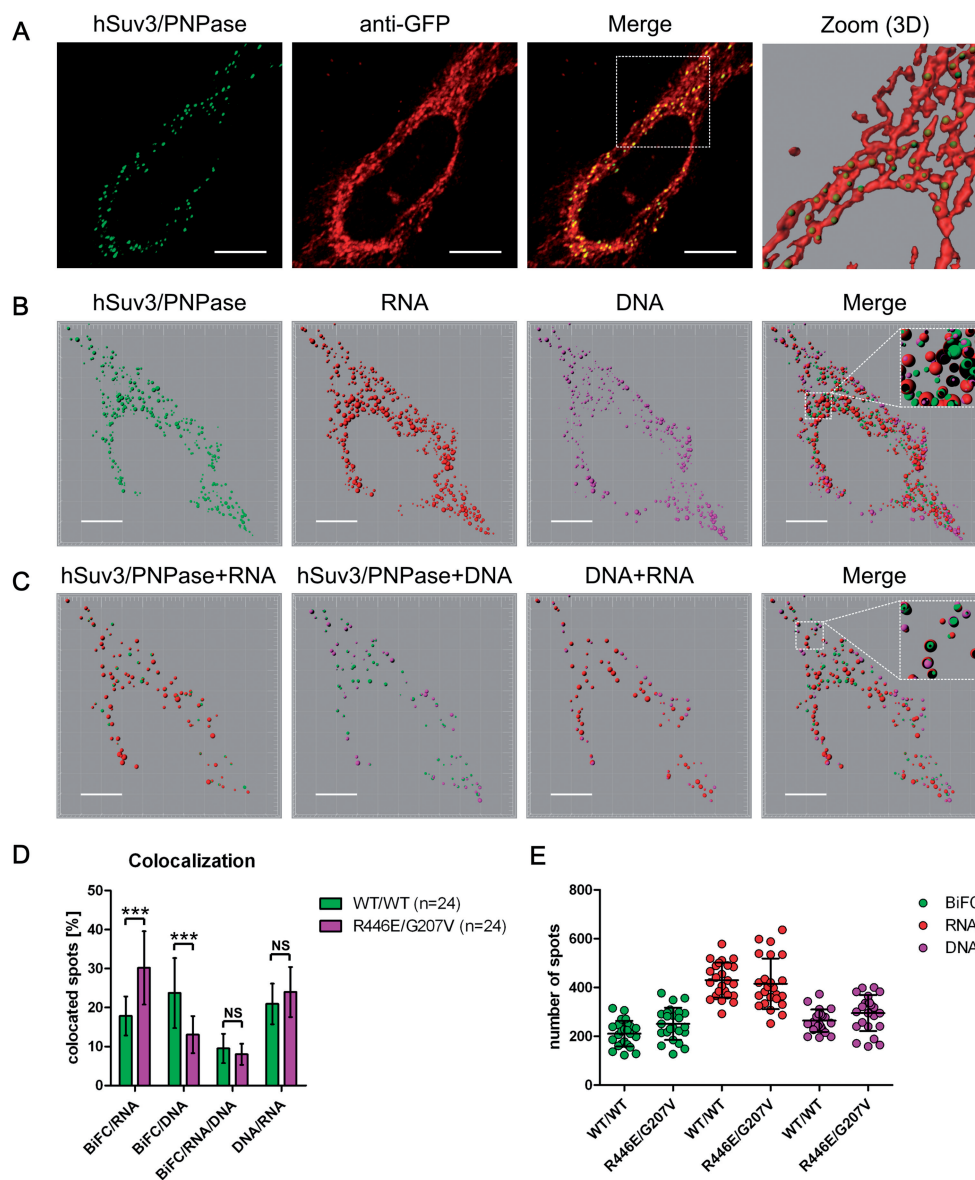
Figure 8. The PNPase–hSuv3 complex is formed in foci and co-localizes with mtRNA and mtDNA. (**A**) The complex of PNPase and hSuv3 was visualized using the BiFC technique by expression of PNPase-C-Venus and hSuv3-N-Venus fusion proteins in HeLa cells. PNPase-C-Venus was stained using specific antibodies anti-GFP. The 3D reconstruction of fluorescence image is presented. The surface of mitochondria was made transparent to visualize PNPase–hSuv3 foci. (**B**) The 3D reconstruction of PNPase–hSuv3 complexes, which were visualized by the BiFC technique, co-localizing with mtRNA and mtDNA. RNA was stained by BrU labeling and appropriate antibodies; DNA was stained using anti-DNA antibodies. The cross-section of the zoomed image is shown, which allows looking inside the objects. (**C**) Images resulting from object-based co-localization studies performed on the image presented in B. Only co-localizing spots are shown. The threshold for co-localization was 0.25 μm, the distance between centers of the objects. (A–C) Bars represent 10 μm. (**D**) Graph representing the mean values of co-localization of the wild-type and inactive (R446E/G207V) PNPase–hSuv3 complex with mtRNA or mtDNA, or both. Co-localization of mitochondrial nucleoids with mtRNA is also shown. The P values obtained in a t-test were <0.0001 (***) or not significant (NS). The standard deviations are shown. (**E**) Graph representing the total numbers of BiFC, mtRNA and mtDNA spots in cells transfected with plasmids encoding wild-type or inactive forms of PNPase (R446E) and hSuv3 (G207V). The mean values and standard deviations are shown. The differences are statistically insignificant.

visualized mitochondrial nucleoids using anti-DNA antibodies. First, we confirmed that our experimental procedure let us detect mtRNA and mtDNA (Supplementary Figure S6). In agreement with previous reports, both mtRNA and mtDNA were observed as spots (Supplementary Figure S6). Then, we performed object-based co-localization studies of the active and inactive form of the mitochondrial degradosome with mtRNA and mtDNA (Figure 8B, C and D). Such

analysis clearly showed that the hSuv3–PNPase complexes co-localize with mtRNA and mtDNA (Figure 8B, C and D). Four classes of the mitochondrial degradosome could be distinguished: co-localized with mtRNA or mtDNA, co-localized both with mtRNA and mtDNA and a fraction of a free complex, which did not co-localize with any detectable mitochondrial nucleic acid. The same number of degradosome classes was observed regardless of whether wild-type or catalytically inactive

PNPase^{R446E} and hSuv3^{G207V} were analyzed (Figure 8D). Approximately 18% of spots containing wild-type PNPase–hSuv3 complexes co-localize exclusively with mtRNA and 24% exclusively with mtDNA, whereas 9.5% of PNPase–hSuv3 foci co-localize both with mtRNA and mtDNA (Figure 8D).

Expression of the degradosome complex containing inactive proteins (PNPase^{R446E} and hSuv3^{G207V}) resulted in the increase in the number of PNPase–hSuv3 dots co-localized only with mtRNA (30%) and the decrease of those co-localized only with mtDNA (13%) (Figure 8D). The amount of PNPase–hSuv3 complex co-localized with both mtRNA and mtDNA did not change significantly. Similarly, the fraction of mtDNA co-localized with mtRNA, as well as the amount of a free complex, was not altered (Figure 8D). Importantly, the differences in co-localization results were not caused by changes in the total numbers of spots because they stay constant regardless of whether the active or mutated form of PNPase–hSuv3 complex was expressed (Figure 8E). Our results suggest that, as in the case of cytoplasmic RNAs (5), mtRNAs may be degraded in specific bodies. The full composition of these bodies and their exact function require further studies.

Silencing of PNPase leads to cell growth inhibition, decreases the levels of mitochondrially encoded COX2 protein and reduces ATP concentration

Finally, we analyzed the effect of PNPase silencing on cell physiology. We found that, similarly to previous studies (29,32), depletion of PNPase leads to impaired cell growth. To determine this, 293 cells were transfected with control siRNA, or two different PNPase-specific siRNAs and cells were counted during the following days. Two days after transfection, we did not observe significant changes in the number of cells between the control cell culture and cultures subjected to transfection with PNPase siRNAs (Figure 9A). A slight decrease in the number of PNPase-depleted cells was observed 4 days after transfection, which is concomitant with the effect on mtRNA metabolism, and became more pronounced later (Figure 9A). Between 6 and 8 days post-transfection with siRNA specific for PNPase, cells stop to grow (Figure 9A). At the same time, we did not observe increased numbers of dead cells, which suggests that cells stopped dividing rather than began dying.

We also investigated whether PNPase silencing alters the levels of subunits of oxidative phosphorylation (OXPHOS) complexes. Four days after siRNA transfection, substantial decrease in the level of mitochondrially encoded COX2 subunit could be observed in PNPase-depleted cells, whereas the levels of nucleus-encoded subunits (SDHB, ATP5A and UQCRC2) were unaffected (Figure 9B). This effect can most probably lead to dysfunction of OXPHOS. Indeed, when we conducted an experiment in which cells were cultured for 8 days after transfection, we observed acidification of the cell culture medium, a hallmark of respiration defect (28,52,53) when PNPase was down-regulated (Supplementary Figure S7). Such an effect on PNPase silencing was also reported by

others (29) and was accompanied by changes in cell morphology and a decrease in cell number (Supplementary Figure S7). Importantly, expression of a recoded *PNPase* gene, encoding wild-type PNPase but resistant to the applied siRNA, reversed these phenotypes (Supplementary Figure S7). We did not observe rescue when catalytically inactive PNPase (R446E) was expressed (Supplementary Figure S7).

It was previously reported that PNPase depletion reduces the level of ATP (29,32). Moreover, it was also found that depletion of ATP by treatment of cells with deoxyglucose and sodium azide affects mitochondrial polyadenylation (32). Thus, it was proposed that PNPase indirectly influences mtRNA metabolism by maintaining correct nucleotide concentration (32). Therefore, we decided to see whether the changes in mtRNA metabolism that we observe on PNPase silencing can result from a decrease in ATP level.

First, we measured the level of ATP. In agreement with previous studies, we found a decrease of ATP levels in mitochondria isolated from cells with silenced PNPase in comparison with control ones (Figure 9C). Then, we tested whether reduction of ATP levels can lead to accumulation of non-coding mtRNA and short mtRNA species, which are characteristic for PNPase silencing. To do so, we treated cells with chemicals affecting ATP production by different mechanisms, including those previously applied by Slomovic and Schuster (32), and examined their influence on mtRNA for different periods of time. Importantly, during the course of the treatment, which lasted 24 h, microscopy observation revealed the cells stayed alive (data not shown). ATP measurement confirmed a reduction of ATP in treated cells (Figure 9D).

Subsequently, RNA isolated from control and ATP-depleted cells was subjected to northern blot analysis with strand-specific probes detecting ND2 mRNA or ND2 mirror RNA. These transcripts were chosen for the test because the ND2 mirror RNA is detectable under normal cellular conditions. The analysis clearly showed that ATP reduction itself does not lead to accumulation of degradation intermediates or non-coding transcripts (Figure 9E), which is a hallmark of PNPase silencing. Thus, we conclude that these changes in mtRNA metabolism are not indirectly caused by alterations in ATP concentration.

DISCUSSION

We demonstrate here that PNPase is the mitochondrial RNase directly involved in mtRNA degradation. We show that PNPase forms an RNA-degrading complex *in vivo* with the helicase hSuv3. The formation of the complex is indispensable for efficient mtRNA decay: a catalytically inactive hSuv3 mutant has a dominant-negative effect and inhibits mtRNA decay, but deletion of a 5-amino acid motif involved in PNPase binding abolishes this effect. The complex, which we have named the mitochondrial degradosome, is formed only in distinct foci, some of which co-localize with mtRNA spots. As the
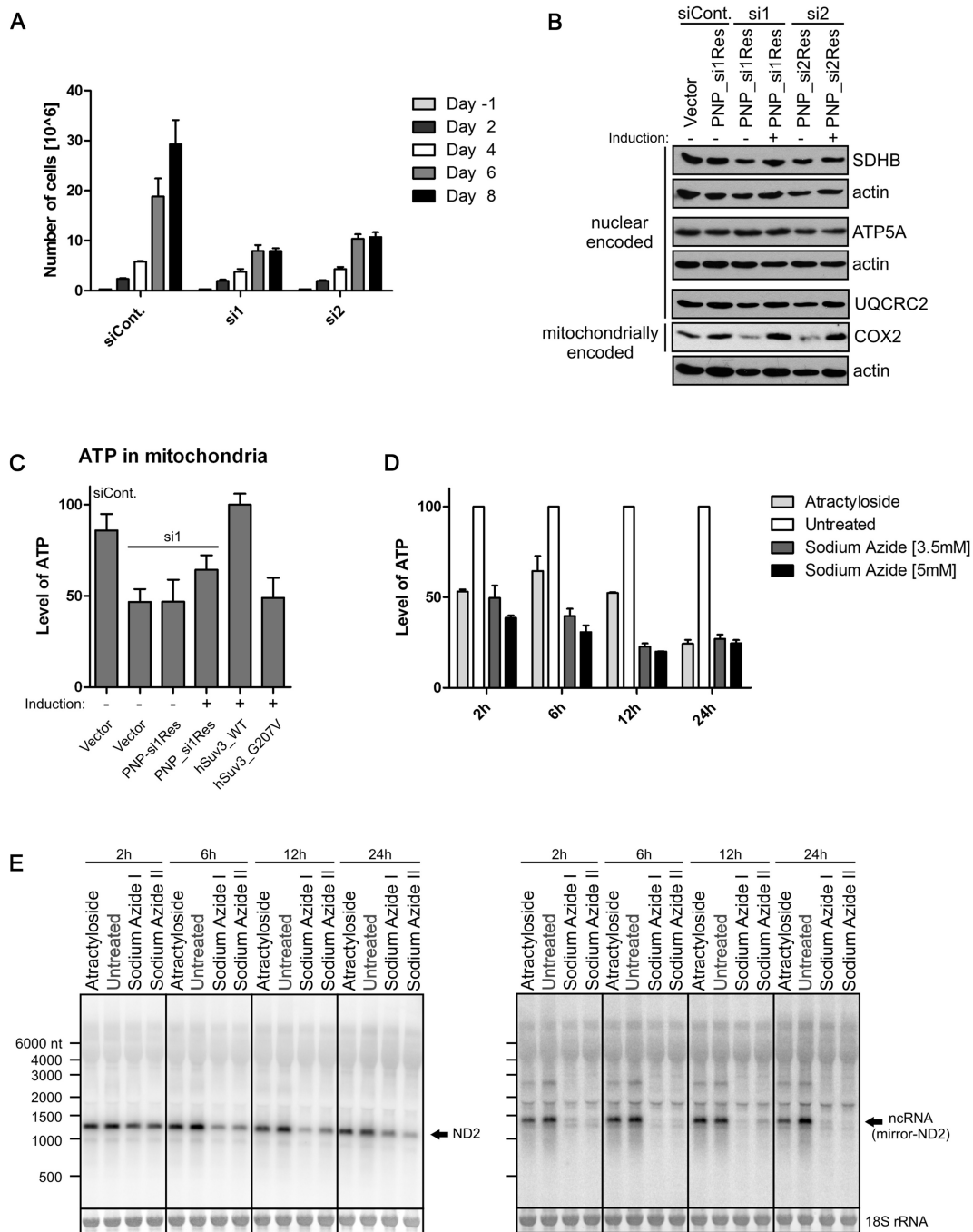
Figure 9. PNPase depletion impairs cell growth, mitochondrial ATP concentration and the level of COX2 protein. (**A**) The inhibition of cell growth on PNPase silencing. 293 T-Rex cells were transfected with siRNA specific for PNPase or negative control siRNA. Cells were counted every 2 days since transfection. Bars represent mean values obtained in three independent experiments; error bars represent standard deviation. (**B**) Western blot analysis of OXPHOS subunits, as standardization actin staining was performed. Stable cell lines (PNP_si1Res, PNP_si2Res) that express inducible PNPase resistant to siRNA anti-PNPase or control cell line having integrated empty vector was transfected with two different siRNAs specific for PNPase (si1 and si2) or control siRNA. (**C**) Quantification of ATP levels in mitochondria after depletion of PNPase. Stable cell line that expresses inducible PNPase resistant to siRNA anti-PNPase and control cell line having integrated empty vector were transfected with siRNA specific for PNPase (si1) or control siRNA. Mitochondria were isolated and ATP levels were analyzed with luminometric assay. As a control, stable cell lines expressing hSuv3 or its catalytically inactive mutant hSuv3_G207V was used. Mean values of three independent experiments are shown; error bars represent standard deviations. (**D**) Quantification of ATP levels in 293 T-Rex cells treated with inhibitors of ATP synthesis. In all cases, culture media were supplemented with 2-deoxy-D-glucose (inhibitor of glycolysis). Cells were treated with atractyloside (blocks ATP-ADP translocase) or two indicated concentrations of sodium azide (inhibits cytochrome oxidase). Cells were collected after 2, 6, 12 and 24 h, and ATP concentrations were analyzed by luminometric assay. Mean values from three independent measurements are presented; error bars represent standard deviations. (**E**) Northern blot analysis of RNA isolated from cells described in C. Strand-specific riboprobes were used. Cytosolic 18S rRNA staining by methylene blue is shown as a loading control.

PNPase–hSuv3 interaction is essential for mtRNA decay and occurs locally, it suggests that degradosome-dependent mtRNA degradation is spatially organized. Nonetheless, the obtained data do not rule out existence of other PNPase/hSuv3- or degradosome-independent mtRNA decay pathways. In particular, the human genome encodes RNases, such as REXO2 or HRSP12, which have been predicted or demonstrated to be targeted to mitochondria [reviewed in (54,55)]. The role of these proteins in mtRNA metabolism, and their potential interplay with PNPase-dependent mtRNA degradation, needs to be challenged experimentally. Thus, although our data show that PNPase is essential for RNA degradation in human mitochondria, it is highly probable that there are also other RNases involved.

Inhibition of RNA degradation should result in increased RNA stability and in the appearance of truncated transcripts, which represent arrested degradation intermediates. Indeed, such changes indicative of participation of PNPase in mtRNA degradation have been observed by us in the case of cells with impaired function of PNPase. We observed a varying impact of PNPase inhibition on the steady-state levels of individual transcripts tested. The mirror RNAs and other normally low abundant non-coding RNAs accumulate strongly, whereas mRNAs, rRNAs and tRNAs are differentially affected. The steady-state levels of some of these RNAs decreased. The exact mechanism responsible for this effect remains to be elucidated. Recently, it was reported that PNPase depletion results in the decrease of mtDNA levels (25), which could explain the decrease in the steady-state levels of some mature mRNAs observed by us. However, in our experimental model, we did not see any changes in mtDNA levels in cells with silenced *PNPase* (Supplementary Figure S8), and therefore, this mechanism cannot be responsible for the decrease of some mt-mRNAs observed by us.

The observed decrease of some transcripts may result from the presence of compensatory mechanism(s) or reflect the fact that individual transcripts may be subjected to diverse control mechanisms. In fact, human mt-mRNAs exhibit more variability as a class than it was previously assumed (55,56). Finally, the observed reduction of mtRNA levels may be a secondary effect of the general deregulation of mitochondrial nucleic acids metabolism, or it may arise from the presence of an alternative RNA decay pathway induced by accumulation of non-coding/spurious RNA. Although it may seem to be contradictory to the proposed role of PNPase in mtRNA decay, such phenomena that dysfunction of RNA decay machinery can lead to decrease of mature transcripts have been previously observed in different cellular compartments in various organisms (34–41). Similarly, decreases in some mature mtRNAs have been observed in yeast harboring mutations in the *SUV3* gene (2,57), which forms a bona fide mitochondrial degradosome with the Dss1 exoribonuclease.

Our results clearly show function of the human degradosome in mtRNA surveillance and decay. We found that PNPase depletion has more pronounced effects on mirror RNAs than mRNAs, which may suggest that the complex is mainly involved in degradation of the former. However, mirror mRNAs seems to have high turnover, as they are hardly detectable under normal physiological conditions. Because of the high turnover rates, they would be especially sensitive to dysfunction of degradation machinery, so we could expect greater effects on these RNAs after PNPase/hSuv3 inactivation. Nonetheless, it may suggest that the complex may be more involved in degradation of mirror RNAs (removal of non-coding RNA and/or RNA surveillance) than in mRNA decay. On the other hand, interesting data were published recently by Chujo *et al.* (25). In addition to the main subject, which is the role of LRPPRC–SLIRP complex in mtRNA stabilization, and in line with our data, this report includes an experiment showing that silencing of the *PNPase* or *hSUV3* genes leads to stabilization of four tested mt-mRNAs (COX1, Cyt B, ATP6/8 and ND5), including Cyt B, which was also analyzed by us. In contrast to the data presented here and our previous report (28), Chujo *et al.* (25) show that depletion of PNPase or hSuv3 leads to almost complete inhibition of mitochondrial mRNA degradation; however, the effect on the steady-state mRNA and non-coding antisense RNA was not reported. This would indicate a crucial role of the PNPase/hSuv3 complex in mt-mRNA decay. Discrepancy between those data and our own regarding the intensity of mt-mRNA stabilization cannot be easily explained. The simplest reasons would be the different cellular models applied (HeLa and 293 used by others and us, respectively) and/or the efficiency of PNPase silencing, which seems to be important for PNPase studies (discussed later). Furthermore, the Suzuki group used a completely different approach to measure stability of mt-mRNAs. They inhibited mtRNA synthesis by treating cells with a high concentration of ethidium bromide and then measured the steady-state levels of mtRNAs using qPCR (25). There are two major issues to consider here. One, ethidium bromide treatment can affect different aspects of the nucleic acid metabolism, for example, mtDNA replication. In our studies, we measured mt-mRNAs half-lives without perturbation of transcription. We used metabolic labeling of RNA with 4sU, which is not toxic and does not affect transcription. This method is currently considered to be the least invasive technique of RNA stability measurement (58). Second, in our approach, we used strand specific riboprobes to detect the investigated transcripts, and we found strong accumulation of antisense transcripts on PNPase depletion; hence, experiments that do not differentiate sense from antisense transcripts may be misleading. Unfortunately, it is not clear whether the others applied strand-specific qPCR in their stability measurement experiments. Importantly, our and Suzuki's (25) reports are the only ones in which stability of mtRNA after PNPase depletion were studied.

Unlike us, Chujo *et al.* (25) found that silencing of PNPase causes mtDNA depletion. This could be also related to a difference in PNPase reduction. Stronger depletion of PNPase may affect mtRNA metabolism stronger and as a consequence lead to mtDNA depletion. This would be in line with evidence of interdependence of RNA metabolism and DNA replication in mammalian

mitochondria (59). Unfortunately, the effectiveness of PNPase depletion performed by us and Chujo *et al.* (25) cannot be directly compared.

Studies of PNPase localization indicated its presence in the IMS while mtRNA is located in the mitochondrial matrix (29). However, as pointed by Chen *et al.* (60), the applied protease-protection method has a detection limit; thus, a small amount of matrix-localized protein may escape detection under some experimental conditions. Indeed, our submitochondrial fractionation (Supplementary Figure S2), co-purification, microscopy and functional studies indicate that a minor fraction of PNPase is localized in the mitochondrial matrix, where it can form a complex with the matrix-localized hSuv3 (61). Thus, it appears that two differentially localized pools of PNPase exist in human mitochondria. Our data, as well as that of others (29), indicate that most of PNPase is in the IMS; however, a smaller fraction of PNPase, which escaped previous identification, also exists in the matrix. Such double submitochondrial localization of PNPase is in agreement with gel filtration chromatography analysis, which distinguished two fractions of hSuv3, one co-migrating with and the other free of PNPase (28). Similarly, in *E. coli*, only a small fraction of PNPase was found in the degradosome (62). Moreover, the formation of the PNPase-RhlB helicase complex, in the absence of RNase E, has also been reported in this organism. This interaction facilitates degradation of dsRNA by bacterial PNPase (63). Such an auxiliary effect was also observed for the PNPase–hSuv3 complex *in vitro* (43).

Our results support the previous reported IMS localization of a major fraction of PNPase and do not contradict its role in RNA import into mitochondria, but they show that the matrix-localized PNPase functions in mtRNA degradation. Cellular tasks played by mammalian PNPase are essential, as the knockout of the mouse *PNPase* gene is embryonically lethal (30). It remains to be determined how the partition of PNPase between the IMS and the matrix is achieved and regulated. Nevertheless, the results of the present and other studies indicate that PNPase appears to play a crucial role in controlling RNA in human mitochondria by acting at different levels: RNA degradation, processing and import (30,32). It seems the RNA degradation activity of PNPase may have substantial importance for cell physiology because it can affect cellular processes by regulating functioning of mitochondria and in addition by taking part in turnover of specific cytoplasmic substrates, such as mRNA for proto-oncogene c-myc and specific miRNAs, such as miRNA-221 (64–66).

The complex of hSuv3 and PNPase exists in specific foci, which we have named D-foci, as they contain the degradosome complex. They can be detected using FLIM-FRET and BiFC techniques. D-foci overlap with mtRNA and/or mtDNA, suggesting that the degradosome may be involved in different functions in mitochondria. One of them is mtRNA degradation; the hypothetical other functions, such as RNA processing and mtDNA replication, need further studies. Co-localization of the degradosome with mtDNA is in agreement with a report

showing the presence of hSuv3 in purified mitochondrial nucleoids (67). Approximately half of PNPase–hSuv3-containing foci were not co-localized with mtRNA or mtDNA. We cannot distinguish whether the non–co-localized D-foci do not contain RNA, or the amount of Br-RNA is too small to be detected. Importantly, we show that the lack of catalytic activity of both mitochondrial degradosome components results in an increase of complex co-localization with mtRNA. This phenomenon is probably caused by stacking of inactive degradosome complexes on RNA substrates.

The question arises why the function of PNPase in human mtRNA decay was not found in silencing experiments other than by Chujo *et al.* (25) and by us. Apparently, depletion of PNPase in earlier analyses resulted in contradictory results, and this subject has been discussed in several review articles (60,64,68–70). In some experiments, it led to changes in mitochondrial morphology, oxygen consumption and mitochondrial membrane potential (29), whereas in others, no such effect was found (31). Nagaike *et al.* (31) showed that silencing of *PNPase* caused elongation of poly(A) tails of all tested transcripts but no changes in steady-state levels of those transcripts were observed, while in other studies, a reduction of PNPase had a varied impact on different mtRNAs (32). In some studies, lack of PNPase resulted in the decrease of mitochondrially encoded proteins (30), whereas others did not observe any perturbations in mitochondrial translation (31,32). It seems that PNPase studies may be particularly sensitive to the degree of its silencing, as well as the applied experimental system. For instance, it was reported that silencing of *PNPase* in 293 cells reduces the levels of all examined transcripts, such as COX1 and COX2 (30), whereas in an earlier work using a similar experimental approach, the same group did not observe any changes in the levels of tested mtRNAs, including COX1 and COX2 (29). In other studies, cell lines with a constitutively silenced *PNPase* gene were used (32). Although this type of system provides very good experimental material, its main drawback is the possibility of compensating effects, which can mask the primary effects. Indeed the authors observed differences in polyadenylation of the COX1 transcript and ATP levels between cells with stably and transiently depleted PNPase, which was explained by the possibility of adaptation and/or compensation mechanisms.

In our research, we used transient silencing of *PNPase* by modified stealthRNAs, which in our experience gave higher efficiency of silencing than the standard siRNAs. Importantly, we confirmed the specificity of the observed phenotypes by rescue experiments in which wild-type but not catalytically inactive PNPase restored mtRNA metabolism. To the best of our knowledge, we are the only group so to date to have confirmed RNAi results by rescue experiments. We are therefore positive that the observed phenotypes are because of PNPase depletion.

In addition, most PNPase studies concerning mtRNA were performed using PCR-based approaches. Although in some cases, it is indispensable (like in cRT-PCR analysis), it does have major drawbacks. The variety of RNA species that can be detected by a given set of PCR

conditions and primers is limited. Also, the occurrence of amplification provides no information about the length of the template molecule because—unless special strategies are used to avoid it—different molecules, such as precursors, mature transcripts and degradation intermediates, can give rise the same PCR product. For these reasons, we used northern hybridizations instead of PCR in our studies. In fact, even using a PCR-based approach, Slomovic and Schuster found truncated transcripts in PNPase-depleted cells, which they regarded as degradation intermediates (32). Again, this is in line with our data.

In conclusion, we show that PNPase and hSuv3 form an RNA-degrading complex in specific D-foci within human mitochondria. Some of D-foci are involved in mtRNA degradation. It remains to be elucidated what other factors, if any, contribute to spatial organization of this process and how mitochondrial transcripts are destined for degradation.

SUPPLEMENTARY DATA

Supplementary Data are available at NAR Online: Supplementary Table 1, Supplementary Figures 1–8, Supplementary Methods and Supplementary Movies 1–5.

ACKNOWLEDGEMENTS

FUNDING

Conflict of interest statement. None declared.

REFERENCES

1. Carpousis,A.J. (2007) The RNA degradosome of *Escherichia coli*: an mRNA-degrading machine assembled on RNase E. *Annu. Rev. Microbiol.*, **61**, 71–87.
2. Dziembowski,A., Piwowarski,J., Hoser,R., Minczuk,M., Dmochowska,A., Siep,M., van der Spek,H., Grivell,L. and Stepien,P.P. (2003) The yeast mitochondrial degradosome. Its composition, interplay between RNA helicase and RNase activities and the role in mitochondrial RNA metabolism. *J. Biol. Chem.*, **278**, 1603–1611.
3. Lykke-Andersen,S., Tomecki,R., Jensen,T.H. and Dziembowski,A. (2011) The eukaryotic RNA exosome: same scaffold but variable catalytic subunits. *RNA Biol.*, **8**, 61–66.
4. Chlebowski,A., Tomecki,R., Lopez,M.E., Seraphin,B. and Dziembowski,A. (2011) Catalytic properties of the eukaryotic exosome. *Adv. Exp. Med. Biol.*, **702**, 63–78.
5. Parker,R. and Sheth,U. (2007) P bodies and the control of mRNA translation and degradation. *Mol. Cell*, **25**, 635–646.
6. Holt,I.J., He,J., Mao,C.C., Boyd-Kirkup,J.D., Martinsson,P., Sembongi,H., Reyes,A. and Spelbrink,J.N. (2007) Mammalian mitochondrial nucleoids: organizing an independently minded genome. *Mitochondrion*, **7**, 311–321.
7. Spelbrink,J.N., Li,F.Y., Tiranti,V., Nikali,K., Yuan,Q.P., Tariq,M., Wanrooij,S., Garrido,N., Comi,G., Morandi,L. *et al.* (2001) Human mitochondrial DNA deletions associated with mutations in the gene encoding Twinkle, a phage T7 gene 4-like protein localized in mitochondria. *Nat. Genet.*, **28**, 223–231.
8. Brzezniak,L.K., Bijata,M., Szczesny,R.J. and Stepien,P.P. (2011) Involvement of human ELAC2 gene product in 3' end processing of mitochondrial tRNAs. *RNA Biol.*, **8**, 616–626.
9. Holzmann,J., Frank,P., Loffler,E., Bennett,K.L., Gerner,C. and Rossmanith,W. (2008) RNase P without RNA: identification and functional reconstitution of the human mitochondrial tRNA processing enzyme. *Cell*, **135**, 462–474.
10. Lopez Sanchez,M.I., Mercer,T.R., Davies,S.M., Shearwood,A.M., Nygard,K.K., Richman,T.R., Mattick,J.S., Rackham,O. and Filipovska,A. (2011) RNA processing in human mitochondria. *Cell Cycle*, **10**, 2904–2916.
11. Ojala,D., Montoya,J. and Attardi,G. (1981) tRNA punctuation model of RNA processing in human mitochondria. *Nature*, **290**, 470–474.
12. Aloni,Y. and Attardi,G. (1971) Symmetrical in vivo transcription of mitochondrial DNA in HeLa cells. *Proc. Natl Acad. Sci. USA*, **68**, 1757–1761.
13. Dmochowska,A., Golik,P. and Stepien,P.P. (1995) The novel nuclear gene DSS-1 of *Saccharomyces cerevisiae* is necessary for mitochondrial biogenesis. *Curr. Genet.*, **28**, 108–112.
14. Malecki,M., Jedrzejczak,R., Stepien,P.P. and Golik,P. (2007) *In vitro* reconstitution and characterization of the yeast mitochondrial degradosome complex unravels tight functional interdependence. *J. Mol. Biol.*, **372**, 23–36.
15. Margossian,S.P., Li,H., Zassenhaus,H.P. and Butow,R.A. (1996) The DExH box protein Suv3p is a component of a yeast mitochondrial 3'-to-5' exoribonuclease that suppresses group I intron toxicity. *Cell*, **84**, 199–209.
16. Stepien,P.P., Margossian,S.P., Landsman,D. and Butow,R.A. (1992) The yeast nuclear gene suv3 affecting mitochondrial post-transcriptional processes encodes a putative ATP-dependent RNA helicase. *Proc. Natl Acad. Sci. USA*, **89**, 6813–6817.
17. Holec,S., Lange,H., Kuhn,K., Alioua,M., Borner,T. and Gagliardi,D. (2006) Relaxed transcription in Arabidopsis mitochondria is counterbalanced by RNA stability control mediated by polyadenylation and polynucleotide phosphorylase. *Mol. Cell Biol.*, **26**, 2869–2876.
18. Mohanty,B.K. and Kushner,S.R. (2000) Polynucleotide phosphorylase functions both as a 3' right-arrow 5' exonuclease and a poly(A) polymerase in *Escherichia coli*. *Proc. Natl Acad. Sci. USA*, **97**, 11966–11971.
19. Leszczyniecka,M., Kang,D.C., Sarkar,D., Su,Z.Z., Holmes,M., Valerie,K. and Fisher,P.B. (2002) Identification and cloning of human polynucleotide phosphorylase, hPNPase old-35, in the context of terminal differentiation and cellular senescence. *Proc. Natl Acad. Sci. USA*, **99**, 16636–16641.
20. Piwowarski,J., Grzechnik,P., Dziembowski,A., Dmochowska,A., Minczuk,M. and Stepien,P.P. (2003) Human polynucleotide phosphorylase, hPNPase, is localized in mitochondria. *J. Mol. Biol.*, **329**, 853–857.

21. Carpousis,A.J. (2002) The *Escherichia coli* RNA degradosome: structure, function and relationship in other ribonucleolytic multienzyme complexes. *Biochem. Soc. Trans.*, **30**, 150–155.

22. Shi,Z., Yang,W.Z., Lin-Chao,S., Chak,K.F. and Yuan,H.S. (2008) Crystal structure of *Escherichia coli* PNPase: central channel residues are involved in processive RNA degradation. *RNA*, **14**, 2361–2371.

23. Symmons,M.F., Jones,G.H. and Luisi,B.F. (2000) A duplicated fold is the structural basis for polynucleotide phosphorylase catalytic activity, processivity, and regulation. *Structure*, **8**, 1215–1226.

24. Lin,C.L., Wang,Y.T., Yang,W.Z., Hsiao,Y.Y. and Yuan,H.S. (2011) Crystal structure of human polynucleotide phosphorylase: insights into its domain function in RNA binding and degradation. *Nucleic Acids Res.*, **40**, 4146–4157.

25. Chujo,T., Ohira,T., Sakaguchi,Y., Goshima,N., Nomura,N., Nagao,A. and Suzuki,T. (2012) LRPPRC/SLIRP suppresses PNPase-mediated mRNA decay and promotes polyadenylation in human mitochondria. *Nucleic Acids Res.*, **40**, 8033–8047.

26. Ruzzenente,B., Metodiev,M.D., Wredenberg,A., Bratic,A., Park,C.B., Camara,Y., Milenkovic,D., Zickermann,V., Wibom,R., Hultenby,K. *et al.* (2012) LRPPRC is necessary for polyadenylation and coordination of translation of mitochondrial mRNAs. *EMBO J.*, **31**, 443–456.

27. Sasarman,F., Brunel-Guitton,C., Antonicka,H., Wai,T. and Shoubridge,E.A. (2010) LRPPRC and SLIRP interact in a ribonucleoprotein complex that regulates posttranscriptional gene expression in mitochondria. *Mol. Biol. Cell*, **21**, 1315–1323.

28. Szczesny,R.J., Borowski,L.S., Brzezniak,L.K., Dmochowska,A., Gewartowski,K., Bartnik,E. and Stepien,P.P. (2010) Human mitochondrial RNA turnover caught in flagranti: involvement of hSuv3p helicase in RNA surveillance. *Nucleic Acids Res.*, **38**, 279–298.

29. Chen,H.W., Rainey,R.N., Balatoni,C.E., Dawson,D.W., Troke,J.J., Wasiak,S., Hong,J.S., McBride,H.M., Koehler,C.M., Teitell,M.A. *et al.* (2006) Mammalian polynucleotide phosphorylase is an intermembrane space RNase that maintains mitochondrial homeostasis. *Mol. Cell Biol.*, **26**, 8475–8487.

30. Wang,G., Chen,H.W., Oktay,Y., Zhang,J., Allen,E.L., Smith,G.M., Fan,K.C., Hong,J.S., French,S.W., McCaffery,J.M. *et al.* (2010) PNPASE regulates RNA import into mitochondria. *Cell*, **142**, 456–467.

31. Nagaike,T., Suzuki,T., Katoh,T. and Ueda,T. (2005) Human mitochondrial mRNAs are stabilized with polyadenylation regulated by mitochondria-specific poly(A) polymerase and polynucleotide phosphorylase. *J. Biol. Chem.*, **280**, 19721–19727.

32. Slomovic,S. and Schuster,G. (2008) Stable PNPase RNAi silencing: its effect on the processing and adenylation of human mitochondrial RNA. *RNA*, **14**, 310–323.

33. Dolken,L., Ruzsics,Z., Radle,B., Friedel,C.C., Zimmer,R., Mages,J., Hoffmann,R., Dickinson,P., Forster,T., Ghazal,P. *et al.* (2008) High-resolution gene expression profiling for simultaneous kinetic parameter analysis of RNA synthesis and decay. *RNA*, **14**, 1959–1972.

34. Chekanova,J.A., Gregory,B.D., Reverdatto,S.V., Chen,H., Kumar,R., Hooker,T., Yazaki,J., Li,P., Skiba,N., Peng,Q. *et al.* (2007) Genome-wide high-resolution mapping of exosome substrates reveals hidden features in the Arabidopsis transcriptome. *Cell*, **131**, 1340–1353.

35. Goeres,D.C., Van Norman,J.M., Zhang,W., Fauver,N.A., Spencer,M.L. and Sieburth,L.E. (2007) Components of the Arabidopsis mRNA decapping complex are required for early seedling development. *Plant Cell*, **19**, 1549–1564.

36. Guan,Q., Zheng,W., Tang,S., Liu,X., Zinkel,R.A., Tsui,K.W., Yandell,B.S. and Culbertson,M.R. (2006) Impact of nonsense-mediated mRNA decay on the global expression profile of budding yeast. *PLoS Genet.*, **2**, e203.

37. He,F., Li,X., Spatrick,P., Casillo,R., Dong,S. and Jacobson,A. (2003) Genome-wide analysis of mRNAs regulated by the nonsense-mediated and 5′ to 3′ mRNA decay pathways in yeast. *Mol. Cell*, **12**, 1439–1452.

38. Kiss,D.L. and Andrulis,E.D. (2010) Genome-wide analysis reveals distinct substrate specificities of Rrp6, Dis3, and core exosome subunits. *RNA*, **16**, 781–791.

39. Rymarquis,L.A., Souret,F.F. and Green,P.J. (2011) Evidence that XRN4, an Arabidopsis homolog of exoribonuclease XRN1, preferentially impacts transcripts with certain sequences or in particular functional categories. *RNA*, **17**, 501–511.

40. Wittmann,J., Hol,E.M. and Jack,H.M. (2006) hUPF2 silencing identifies physiologic substrates of mammalian nonsense-mediated mRNA decay. *Mol. Cell Biol.*, **26**, 1272–1287.

41. Yepiskoposyan,H., Aeschimann,F., Nilsson,D., Okoniewski,M. and Muhlemann,O. (2011) Autoregulation of the nonsense-mediated mRNA decay pathway in human cells. *RNA*, **17**, 2108–2118.

42. Portnoy,V., Palnizky,G., Yehudai-Resheff,S., Glaser,F. and Schuster,G. (2008) Analysis of the human polynucleotide phosphorylase (PNPase) reveals differences in RNA binding and response to phosphate compared to its bacterial and chloroplast counterparts. *RNA*, **14**, 297–309.

43. Wang,D.D., Shu,Z., Lieser,S.A., Chen,P.L. and Lee,W.H. (2009) Human mitochondrial SUV3 and polynucleotide phosphorylase form a 330-kDa heteropentamer to cooperatively degrade double-stranded RNA with a 3′-to-5′ directionality. *J Biol Chem*, **284**, 20812–20821.

44. Dziembowski,A. and Seraphin,B. (2004) Recent developments in the analysis of protein complexes. *FEBS Lett.*, **556**, 1–6.

45. Bastiaens,P.I. and Squire,A. (1999) Fluorescence lifetime imaging microscopy: spatial resolution of biochemical processes in the cell. *Trends Cell Biol.*, **9**, 48–52.

46. Wallrabe,H. and Periasamy,A. (2005) Imaging protein molecules using FRET and FLIM microscopy. *Curr. Opin. Biotechnol.*, **16**, 19–27.

47. Shyu,Y.J., Liu,H., Deng,X. and Hu,C.D. (2006) Identification of new fluorescent protein fragments for bimolecular fluorescence complementation analysis under physiological conditions. *Biotechniques*, **40**, 61–66.

48. Hu,C.D., Chinenov,Y. and Kerppola,T.K. (2002) Visualization of interactions among bZIP and Rel family proteins in living cells using bimolecular fluorescence complementation. *Mol. Cell*, **9**, 789–798.

49. Khidr,L., Wu,G., Davila,A., Procaccio,V., Wallace,D. and Lee,W.H. (2008) Role of SUV3 helicase in maintaining mitochondrial homeostasis in human cells. *J. Biol. Chem.*, **283**, 27064–27073.

50. Szczesny,R.J., Obriot,H., Paczkowska,A., Jedrzejczak,R., Dmochowska,A., Bartnik,E., Formstecher,P., Polakowska,R. and Stepien,P.P. (2007) Down-regulation of human RNA/DNA helicase SUV3 induces apoptosis by a caspase- and AIF-dependent pathway. *Biol. Cell*, **99**, 323–332.

51. Iborra,F.J., Kimura,H. and Cook,P.R. (2004) The functional organization of mitochondrial genomes in human cells. *BMC Biol.*, **2**, 9.

52. Jazayeri,M., Andreyev,A., Will,Y., Ward,M., Anderson,C.M. and Clevenger,W. (2003) Inducible expression of a dominant negative DNA polymerase-gamma depletes mitochondrial DNA and produces a rho0 phenotype. *J. Biol. Chem.*, **278**, 9823–9830.

53. Rorbach,J., Nicholls,T.J. and Minczuk,M. (2011) PDE12 removes mitochondrial RNA poly(A) tails and controls translation in human mitochondria. *Nucleic Acids Res.*, **39**, 7750–7763.

54. Bruni,F., Gramegna,P., Lightowlers,R.N. and Chrzanowska-Lightowlers,Z.M. (2012) The mystery of mitochondrial RNases. *Biochem. Soc. Trans.*, **40**, 865–869.

55. Rorbach,J. and Minczuk,M. (2012) The post-transcriptional life of mammalian mitochondrial RNA. *Biochem. J.*, **444**, 357–373.

56. Temperley,R.J., Wydro,M., Lightowlers,R.N. and Chrzanowska-Lightowlers,Z.M. (2010) Human mitochondrial mRNAs–like members of all families, similar but different. *Biochim. Biophys. Acta*, **1797**, 1081–1085.

57. Golik,P., Szczepanek,T., Bartnik,E., Stepien,P.P. and Lazowska,J. (1995) The *S. cerevisiae* nuclear gene SUV3 encoding a putative RNA helicase is necessary for the stability of mitochondrial transcripts containing multiple introns. *Curr. Genet.*, **28**, 217–224.

58. Balagopal,V., Fluch,L. and Nissan,T. (2012) Ways and means of eukaryotic mRNA decay. *Biochim. Biophys. Acta*, **1819**, 593–603.

59. Kasiviswanathan,R., Collins,T.R. and Copeland,W.C. (2012) The interface of transcription and DNA replication in the mitochondria. *Biochim. Biophys. Acta*, **1819**, 970–978.

60. Chen,H.W., Koehler,C.M. and Teitell,M.A. (2007) Human polynucleotide phosphorylase: location matters. *Trends Cell Biol.*, **17**, 600–608.

61. Minczuk,M., Piwowarski,J., Papworth,M.A., Awiszus,K., Schalinski,S., Dziembowski,A., Dmochowska,A., Bartnik,E., Tokatlidis,K., Stepien,P.P. *et al.* (2002) Localisation of the human hSuv3p helicase in the mitochondrial matrix and its preferential unwinding of dsDNA. *Nucleic Acids Res.*, **30**, 5074–5086.

62. Liou,G.G., Jane,W.N., Cohen,S.N., Lin,N.S. and Lin-Chao,S. (2001) RNA degradosomes exist in vivo in *Escherichia coli* as multicomponent complexes associated with the cytoplasmic membrane via the N-terminal region of ribonuclease E. *Proc. Natl Acad. Sci. USA*, **98**, 63–68.

63. Liou,G.G., Chang,H.Y., Lin,C.S. and Lin-Chao,S. (2002) DEAD box RhlB RNA helicase physically associates with exoribonuclease PNPase to degrade double-stranded RNA independent of the degradosome-assembling region of RNase E. *J. Biol. Chem.*, **277**, 41157–41162.

64. Das,S.K., Bhutia,S.K., Sokhi,U.K., Dash,R., Azab,B., Sarkar,D. and Fisher,P.B. (2011) Human polynucleotide phosphorylase (hPNPase(old-35)): an evolutionary conserved gene with an expanding repertoire of RNA degradation functions. *Oncogene*, **30**, 1733–1743.

65. Das,S.K., Sokhi,U.K., Bhutia,S.K., Azab,B., Su,Z.Z., Sarkar,D. and Fisher,P.B. (2010) Human polynucleotide phosphorylase selectively and preferentially degrades microRNA-221 in human melanoma cells. *Proc. Natl Acad. Sci. USA*, **107**, 11948–11953.

66. Sarkar,D., Leszczyniecka,M., Kang,D.C., Lebedeva,I.V., Valerie,K., Dhar,S., Pandita,T.K. and Fisher,P.B. (2003) Down-regulation of Myc as a potential target for growth arrest induced by human polynucleotide phosphorylase (hPNPaseold-35) in human melanoma cells. *J. Biol. Chem.*, **278**, 24542–24551.

67. Wang,Y. and Bogenhagen,D.F. (2006) Human mitochondrial DNA nucleoids are linked to protein folding machinery and metabolic enzymes at the mitochondrial inner membrane. *J. Biol. Chem.*, **281**, 25791–25802.

68. Borowski,L.S., Szczesny,R.J., Brzezniak,L.K. and Stepien,P.P. (2010) RNA turnover in human mitochondria: more questions than answers? *Biochim. Biophys. Acta*, **1797**, 1066–1070.

69. Nagaike,T., Suzuki,T. and Ueda,T. (2008) Polyadenylation in mammalian mitochondria: insights from recent studies. *Biochim. Biophys. Acta*, **1779**, 266–269.

70. Schuster,G. and Stern,D. (2009) RNA polyadenylation and decay in mitochondria and chloroplasts. *Prog. Mol. Biol. Transl. Sci.*, **85**, 393–422.